Kinetics of charge translocation in the passive downhill uptake mode of the Na$^+$/H$^+$ antiporter NhaA of *Escherichia coli*

D. Zuber[a], R. Krause[b], M. Venturi[a,1], E. Padan[c], E. Bamberg[a], K. Fendler[a,*]

[a]*Max Planck Institut für Biophysik, Max von Laue Strasse 3, D-60438 Frankfurt/Main, Germany*
[b]*IonGate Biosciences GmbH, Frankfurt/Main, Germany*
[c]*Institute of Life Sciences, Hebrew University of Jerusalem, 91904 Jerusalem, Israel*

Abstract

The Na$^+$/H$^+$ antiporter NhaA is the main Na$^+$ extrusion system in *E. coli*. Using direct current measurements combined with a solid supported membrane (SSM), we obtained electrical data of the function of NhaA purified and reconstituted in liposomes. These measurements demonstrate NhaA's electrogenicity, its specificity for Li$^+$ and Na$^+$ and its pronounced pH dependence in the range pH 6.5–8.5. The mutant G338S, in contrast, presents a pH independent profile, as reported previously. A complete right-side-out orientation of the NhaA antiporter within the proteoliposomal membrane was determined using a NhaA-specific antibody based ELISA assay. This allowed for the first time the investigation of NhaA in the passive downhill uptake mode corresponding to the transport of Na$^+$ from the periplasmic to the cytoplasmic side of the membrane. In this mode, the transporter has kinetic properties differing significantly from those of the previously investigated efflux mode. The apparent K_m values were 11 mM for Na$^+$ and 7.3 mM for Li$^+$ at basic pH and 180 mM for Na$^+$ and 50 mM for Li$^+$ at neutral pH. The data demonstrate that in the passive downhill uptake mode pH regulation of the carrier affects both apparent K_m as well as turnover (V_{max}).

1. Introduction

Sodium proton antiporters [1] are ubiquitous membrane proteins found in the cytoplasmic and organelle membranes of cells of many different origins, including plants, animals and microorganisms. They are involved in cell energetics, and play primary roles in the regulation of intracellular pH, cellular Na$^+$ content and cell volume (reviews in [2–5]).

NhaA, the main Na$^+$/H$^+$ antiporter in *Escherichia coli*, is indispensable for adaptation to high salinity, for challenging Li$^+$ toxicity, and for growth at alkaline pH (in the presence of Na$^+$) [2,6–8]. It is widely spread in enterobacteria and has orthologues in many other prokaryotes.

NhaA is an electrogenic antiporter which has been purified to homogeneity and reconstituted in a functional form in proteoliposomes [8,9]. One of the most interesting characteristics of NhaA is its dramatic dependence on pH, a property it shares with both prokaryotic [10] and eukaryotic antiporters [3–5]. The activity of NhaA changes over three orders of magnitude between pH 6.5 and pH 8.5 [2,9]. Amino acid residues involved in the pH response of NhaA have been characterized. Out of the eight histidines of NhaA only His225 is essential for the pH response of the antiporter [11,12]. Replacement of Gly 338 with serine (G338S) produces a transporter which in contrast to the wild-type

protein lacks pH control; it is active throughout the pH range between pH 6.5 and 8.5 [13]. Residues clustering in the N-terminus and loop VIII-IX of NhaA also affect the pH regulation of NhaA [10]. The most dramatic effect is that of E252C that causes an alkaline shift of one pH unit [14]. Remarkably, cross-linking data show that these two segments of NhaA are in close proximity [10,15].

NhaA undergoes a conformational change upon its activation by pH which can be probed by trypsin [16,17]. In everted membrane vesicles as well as in DDM micelles, NhaA is completely resistant to trypsin at acidic pH, while at alkaline pH, it is digested at Lys249, in a pattern reflecting the pH profile of the antiporter activity. The conformational change has recently been monitored by a fluorescent probe at position E252C [14].

A monoclonal antibody (mAb 1F6) was raised against the NhaA antiporter [18]. This mAb recognizes yet another domain of NhaA which responds to pH [19]. The antibody binds NhaA at pH 8.5, but not at pH 4.5. The epitope of mAb 1F6 was located at the N-terminus of NhaA [19].

Transport studies of the purified NhaA reconstituted in proteoliposomes showed that its stoichiometry is 2 H^+ for 1 Na^+ [20]. Nevertheless, similar to all ion-coupled transporters neither its molecular mechanism nor its partial reactions have been elucidated.

Recently, applying electrophysiology opened new avenues to the study of the mechanism of active transport. Measuring currents in membrane patches of *Xenopus* oocytes expressing neurotransmitter transporters revealed the existence of channel like currents accompanying the transport reaction [21–25]. These data have suggested the intriguing possibility that the mechanism of channels and carriers need not necessarily be mutually exclusive [25].

None of the sodium-proton antiporters have as yet been subjected to electrophysiological studies. In the present work, we measured transient electrical currents in the millisecond time range generated by the NhaA antiporter using a technique which has been previously applied to numerous electrogenic ion pumps [26–28] and recently also to secondary transporters [29]. Investigation of the orientation of the NhaA carrier reconstituted in liposomes showed that NhaA is reconstituted predominantly in RSO (right side out) orientation. Therefore, the observed electric activity of NhaA allowed the study of the properties of the passive downhill uptake mode of the carrier.

2. Materials and methods

2.1. His-tagged NhaA Na^+/H^+ exchanger overproduction and purification

His-tagged NhaA Na^+/H^+ exchanger (His-NhaA) was engineered [30], overproduced in *E. coli* and purified on a

Ni^{2+}-NTA column as previously reported [8]. His-tagged NhaA is a dimer when solubilized in DDM before reconstitution [18].

2.2. Reconstitution of purified His-NhaA into liposomes

The reconstitution process was performed in three steps: (1) preparation of lipids: The total *E. coli* lipids extract (50% PE) was dissolved in chloroform (20 mg/ml) and 0.5–1.0 ml were gently dried in a glass tube with a rotational evaporator under a nitrogen stream at room temperature. The lipid film on the bottom of the glass tube was incubated with a buffer solution (100 mM Tris, 100 mM Mops, 100 mM HEPES, 50 mM KCl, 10 mM $MgCl_2$, 10 mg/ml DDM, titrated to pH 8.0 with KOH) for at least 1 h and was gently shaken until the lipid film was completely dissolved to yield a 10 mg/ml lipids buffer solution. The solution was sonicated in a strong bath type sonicator for at least 1 min until looking almost clear. (2) Solubilized His–NhaA was added in a mass ratio of 1:3–1:500 to the lipid content (lipid to protein ratio LPR = 3–500). The solution was vortexed and incubated on ice for at least 15 min. (3) Removal of the detergent was accomplished by the addition of polystyrene beads (Bio-Beads, Bio-Rad) in a volume ratio of approximately 1:3. The solution was either shaken or gently stirred with a magnetic stirrer over night at 7 °C. Then, the bio-beads were exchanged for fresh ones in a volume ratio of approximately 1:5 and the solution was stirred for 1 h. After removal of the bio-beads the solution was centrifuged at $10^4 \times g$ for 6 min and the small pellet was discarded, while aliquots of the supernatant were frozen in liquid nitrogen and stored at −80 °C. Reconstitution was verified by freeze fracture electron microscopy. From the microscopic images, it was estimated that the protein density was approximately 100 times lower in LPR = 500 than in LPR = 10 proteoliposomes. Prior to use, the samples were thawed on ice and gently sonicated for 2–5 s.

2.3. Expression and purification of F_v-2C5 fragment

NhaA-specific mAb, 2C5, has previously been isolated and described [18]. To clone the DNA that encodes the mAb F_v fragment 2C5, total RNA was extracted from the mAb 2C5 producing hybridoma clone, using the RNeasy kit (Qiagen, Hilden, Germany). After reverse transcription with oligo-d(T), the DNA sequence encoding the F_v-2C5 fragment was cloned into pASK68 expression vector. The protein fused to a strep-tag was produced in *E. coli* JM83 strain and purified on a streptavidin column as previously described [31].

2.4. Binding assay of F_v-2C5 to NhaA proteoliposomes

Three samples were mixed with F_v-2C5 in a 1:5 molar ratio in 200 µl of buffered saline solution (100 mM K_2HPO_4, 50 mM KH_2PO_4, 50 mM NaCl, pH 7.2) and

incubated for 40 min at 20 °C before the binding assay: (1) NhaA solution that was used for reconstitution=100%. (2) An aliquot of the proteoliposomes for estimation of the total amount of NhaA in the proteoliposomes which is capable of binding the F_v. Therefore, Triton X-100 (2%, v/v) was added to this aliquot before the incubation to solubilize the proteoliposomes and excess F_v was not removed before the binding assay. (3) An identical proteoliposome aliquot for estimation of the amount of NhaA in intact proteoliposomes which binds the F_v. These proteoliposomes, after incubation with the F_v, were washed free of excess F_v (three washes by centrifugation at 30,000 g followed by re-suspension in the buffer) and solubilized in the buffer containing Triton X-100 before the binding assay.

The binding assay was based on the strep-tag affinity tag of F_v-2C5 using a strep-tag based ELISA assay for quantization of the complex NhaA-F_v-2C5 bound to the plate through the F_v fragment. Each sample was incubated with a streptavidin coated ELISA plate (Qiagen). The binding buffer contained: 20 mM Tris/HCl pH 8.0, 100 mM KCl, 0.03% (w/v) DDM (Calbiochem), 0.1% (w/v) bovine serum albumin. Binding was allowed to proceed for 2 h at 20 °C. All other washing steps and incubation with secondary antibodies were done in the same buffer essentially as described in [18]. Finally, the monoclonal antibody 1F6 which binds to the N-terminus of NhaA [19] was used to quantify the complex NhaA-F_v-2C5 bound to the plate through the F_v fragment. An anti-mouse IgG (whole-molecule) alkaline phosphatase conjugated antibody (Sigma) was used in the detection assay. The optical density at 405–450 nm was measured using an ELISA reader. A 1:1 stoichiometric complex of NhaA-F_v-2C5 was used to generate a calibration curve for the signals. Control experiments with NhaA-free liposomes did not give any significant signal.

2.5. Fluorescence measurements

Fluorescence measurements were performed with a Hitachi F4500 fluorescence photo-spectrometer in the time scan configuration, with excitation wavelength 651 nm, emission wavelength 675 nm and slit setting to 5 nm. The fluorescent emission light was filtered with an additional 670 nm long pass filter in the emission pathway. The integration time of the signal detection unit was set to 0.5 s. For the fluorescence measurements, 10 μl of NhaA proteoliposomes were added to 1 ml of the buffer solution in a 2-ml fluorescence cuvette. The solution was stirred during the measurement.

2.6. SSM measurements

The SSM measurement was performed as described previously [28,29]. Briefly, thawed and sonicated NhaA proteoliposomes were allowed to adsorb to an octadecane-thiol/phospholipid hybrid bilayer on a gold surface and the transport process was initiated by a rapid solution exchange (time resolution 10–20 ms). The data sets were recorded either using a home made SSM set-up or with a commercial SURFE^{2}R-1 instrument (IonGate Biosciences, Frankfurt, Germany). A comparison showed that the results generated with the two different instruments were essentially the same.

A single SSM measurement was performed in 3 steps of 0.5 to 1 s duration which differed in the solution present in the SSM cuvette: a nonactivating solution (which did not contain a substrate for the NhaA exchanger), then an activating solution (which contained a substrate) followed by the nonactivating solution. Currents were recorded throughout the whole measurement. They were amplified with a current amplifier set to a gain of $10^9–10^{10}$ V/A and low pass filtering set to 300–1000 Hz.

To prevent artifacts, the substrate cation (Na^+ or Li^+) in the activating solution was replaced by an equal amount of an inert cation (K^+ or choline$^+$) in the nonactivating solution. In addition, the ionic strength was kept high by adding choline$^+$ or K^+ to a total added cation concentration of 240–300 mM. An exception is the inhibition experiment using the F_v-2C5 mAb fragment where low ionic strength was required for binding of the mAb. The detailed composition of the solutions is given in the figure legends.

3. Results

3.1. Fluorescent measurement of the membrane potential created by NhaA in proteoliposomes

Functional activity of the reconstituted His-NhaA (hitherto NhaA) was assessed by steady state fluorescence measurements, using the cationic dye DiSC$_3$ [32] as a probe of membrane potential across the proteoliposome membrane. In the presence of a membrane potential, negative inside, DiSC$_3$ redistributes between the aqueous phase and the liposomal membrane and the fluorescence intensity is quenched as a function of the magnitude of the membrane potential [32,33].

A typical experiment is summarized in Fig. 1: After the addition of 1 μM DiSC$_3$ into the measurement cuvette containing NhaA proteoliposomes in a medium with no added Na^+, the proteoliposome solution was allowed to equilibrate until a stable level of fluorescence was reached. Then, 100 mM Na^+ was added which caused a drastic decrease in the fluorescence signal, indicating the generation of a negative-inside electrical potential. The addition of 20 μM of the protonophore 1799 together with 20 μM of the Na^+/H^+-exchanger monensin restored almost completely the original level of the fluorescence intensity, verifying that the changes observed in the fluorescence intensity were due to the build up of an electrical potential. The detected signal corresponds to an outward directed current and demonstrates the electrogenicity of NhaA, in accordance with the
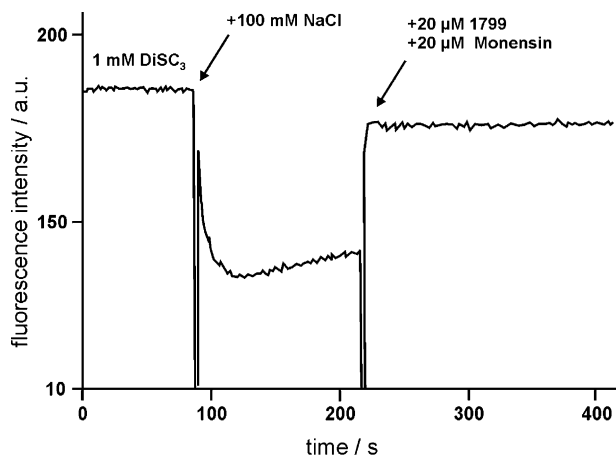
Fig. 1. Fluorescence assay of NhaA activity in proteoliposomes. The fluorescence emission of the dye DiSC$_3$ was used to monitor the electrical potential (negative inside) of NhaA proteoliposomes. DiSC$_3$ (1 μM) was added to the cuvette containing NhaA proteoliposomes (20 μl, 8.75 mg/ml lipids, LPR=17.5) in 1 ml buffer solution (50 mM cholineCl, 0.5 mM NaCl, 1 mM DTT, 25 mM Tris, 25 mM HEPES, pH 8.0) and incubation continued until steady state of fluorescence was reached. Then, 100 mM NaCl was added followed by the ionophores 1799 (20 μM) and monensin (200 μM) as indicated. Excitation and emission wavelengths were 651 nm and 675 nm respectively.

previously measured Na$^+$/2H$^+$ antiport stoichiometry of NhaA [34]. The decay time of the signal is in the order of 100 s (Fig. 1). This indicates that the proteoliposomes are sufficiently impermeable to monovalent cations on a time scale of several seconds, a property crucial for performing electrical current measurements with the SSM technique.

3.2. Orientation of NhaA in the proteoliposomes

It was also crucial for the interpretation of the electric measurements to determine the orientation, whether random or uniform, of NhaA in the proteoliposomes. For this purpose, we used two known topological markers of NhaA. One was the epitope of mAb 2C5, a NhaA-specific mAb [18] that was previously shown to bind to NhaA at the periplasmic side of RSO membrane vesicles [35]. The other was a double factor-Xa protease specific cleavable site that was engineered in the C-terminus of NhaA followed by a His-tag [30]. We have previously shown that the C-terminus of NhaA faces the cytoplasmic side of RSO membrane vesicles [30,36].

The fraction of NhaA in proteoliposomes which binds F$_v$-2C5, reflects the fraction of NhaA that has been reconstituted in RSO orientation. To determine this fraction we used a strep-tag based ELISA. Three samples were processed in parallel: (1) A solution of the purified NhaA (used for the reconstitution) incubated in the presence of excess F$_v$ and then applied to the strep-tag ELISA assay=total amount of NhaA in the system. (2) NhaA proteoliposomes solubilized with 0.3% Triton X-100, incubated with F$_v$-2C5 and processed as above=total amount of reconstituted NhaA. (3) Intact proteoliposomes incubated with the F$_v$ and then washed free of unbound F$_v$. An aliquot of the washed

proteoliposomes solubilized with Triton X-100 was applied to the strep-tag ELISA assay=amount of NhaA reconstituted in RSO orientation.

The ELISA dilution curve of each of the three samples was analyzed by fitting of the data to an adsorption isotherm (Fig. 2A) yielding the respective apparent half saturating constants of the three samples $r_{0.5,i}$ (i=1,2,3). The ratio of any two original concentrations c_i and c_j of samples i and j can be calculated from the experimentally determined apparent half saturating constants $r_{0.5,i}$ and $r_{0.5,j}$, respectively: $c_i/c_j=r_{0.5,j}/r_{0.5,i}$. This yields the degree of reconstitution $c_2/c_1=r_{0.5,1}/$
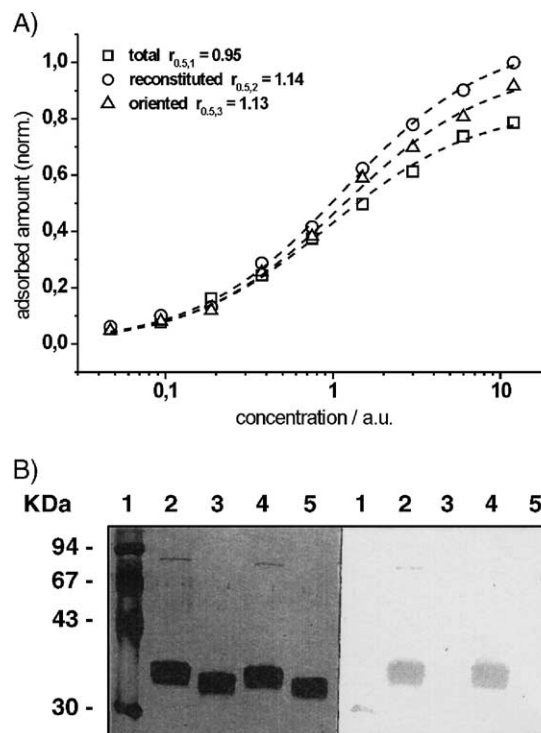

Fig. 2. Orientation of NhaA reconstituted in liposomes. (A) F$_v$-2C5 binding to NhaA reconstituted in proteoliposomes. The proteoliposome solution contained 7.5 mg/ml lipids (LPR=5). ELISA absorption read outs of dilution series of three samples are shown: (□), Total NhaA used for reconstitution incubated with F$_v$-2C5 before the ELISA assay=100%. (○), NhaA proteoliposomes solubilized in 0.3% (v/v) Triton-X100 and incubated with F$_v$-2C5 before the ELISA assay=Total NhaA in proteoliposomes. (△), Intact NhaA proteoliposomes incubated with F$_v$-2C5, washed free of unbound F$_v$-2C5 and solubilized in 0.3% Triton X-100 before the ELISA assay=NhaA in RSO orientation in proteoliposomes. Each experiment was repeated at least three times. The results were normalized to the maximal value obtained with all three preparations. For further details, see Materials and methods. The dashed curves are fits using an adsorption isotherm with the half saturation concentration $r_{0.5,i}$ (i=1, 2, 3). (B) Factor Xa cleavage of the C-terminal histidine-tagged NhaA. Proteoliposomes with an engineered NhaA containing two factor Xa cleavable sites followed by a His-tag at the C-terminus were used. The proteoliposomes were subjected to factor Xa cleavage and the products (1 μg in each sample) were resolved on SDS-PAGE (left panel, silver stained) or Western analysis using anti-His mAb (right panel). In both panels, the gel lanes contained: (1) molecular weight markers, (2) untreated His-tagged NhaA, (3) His-tagged NhaA treated with factor Xa, (4) His-tagged NhaA proteoliposomes treated with factor Xa, (5) His-tagged NhaA proteoliposomes first treated with Triton X-100 and then with factor Xa.
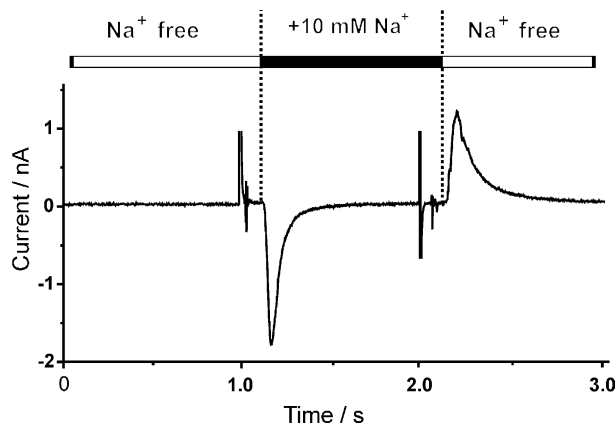
Fig. 3. Electrical current generated by NhaA on the SSM. A 10 mM Na$^+$ concentration jump was performed on NhaA proteoliposomes adsorbed to the SSM. The solution exchange protocol consisted of three subsequent 1s flow steps (flow rate ~1 ml/s) as indicated. For adsorption of proteoliposomes to the SSM, 20 μl of NhaA proteoliposome solution (5 mg/ml lipids, LPR = 3.3) was added to the cuvette. The buffer solution contained 290 mM KCl, 1 mM DTT, 25 mM Tris, 25 mM Mops, 25 mM HEPES, pH 8.0 (Tris). In addition, the nonactivating solution contained 10 mM KCl, the activating solution 10 mM NaCl.

$r_{0.5,2}$ and the degree of RSO orientation $c_3/c_2 = r_{0.5,2}/r_{0.5,3}$. The results summarized in Fig. 2A show that 83% (±7%) of the amount of NhaA added to the reconstitution mixture were found in the final proteoliposome preparation, implying that the reconstitution protocol used is very efficient. Furthermore, 100% (±3%) of the reconstituted NhaA was found in RSO orientation.

Given the RSO orientation of NhaA found in the proteoliposomes, the factor Xa cleavable sites were not expected to be accessible in intact NhaA proteoliposomes but accessible in detergent solubilized proteoliposomes. To test these alternatives, detergent solubilized and intact NhaA proteoliposomes were each subjected to the site-specific factor Xa proteolysis and the products separated on SDS-PAGE (Fig. 2B, left panel). In parallel, identical reaction mixtures were subjected to Western analysis using specific anti-His-tag mAb (Fig. 2B, right panel). The detergent solubilized intact His-NhaA that was used as a control was specifically cleaved by factor Xa protease resulting in a shorter fragment (Fig. 2B, left panel, compare lanes 2 and 3). Accordingly, while the anti-His-tag mAb recognized intact His-NhaA, the proteolytic product was not recognized by the mAb (Fig. 2B, right panel, compare lanes 2 and 3). In marked contrast, NhaA in intact proteoliposomes was resistant to factor Xa cleavage (Fig. 2B, left panel, lane 4) unless previously solubilized in Triton X-100 (Fig. 2B, left panel, lane 5). Accordingly, Western analysis with an anti-His-tag mAb detected NhaA in the former but not in the latter reaction mixture. (Fig. 2B, right panel, compare lanes 4 and 5). Hence, the C-terminal tail of NhaA is protected in the intact proteoliposomes, an observation that agrees with the RSO orientation of NhaA in proteoliposomes.

3.3. Transient currents generated by the NhaA antiporter after a Na$^+$ concentration jump

For activation of NhaA, a concentration jump of the substrates of NhaA, either Na$^+$ or Li$^+$ (in the activating solution) was used. A typical concentration jump experiment is described in Fig. 3: In the first step, the SSM was rinsed with the nonactivating solution for 1 s. Switching to the activating solution that contained 10 mM Na$^+$ elicited a transient "on-signal" (Fig. 3) that lasted for several ms. After 1 s of activating solution, switching back to the nonactivating solution led to an inverted current signal, the "off-signal". In this article, we consider exclusively the on-signal since the off-signal is driven not only by concentration differences but also by the electrochemical potential difference that was created during the activation phase. The time course of the on-signal was characterized by two distinct phases: a fast rise followed by a slow decay. The rising phase of the signal starts when the substrate arrives at the membrane surface which takes place within 10–30 ms after switching of the valves (Fig. 3). The risetime of the signal is 3–10 ms. The decay of the signal can be characterized by two specific decay time constants in the range of 20–500 ms.

3.4. Cation specificity

Current measurements were performed at pH 8.0 using a 10 mM concentration jump of the monovalent cations Li$^+$, Na$^+$, K$^+$ or Rb$^+$ (Fig. 4). Na$^+$ and Li$^+$ generate a peak current of approximately the same size under these conditions, indicating that Na$^+$ and Li$^+$ are transported with the same turnover rates (see concentration-dependent measurements below). However, the signal of Li$^+$ starts earlier and rises faster than that of Na$^+$, which indicates that Li$^+$ is transported with lower apparent K_m than Na$^+$. The current signals reveal a pronounced specificity for
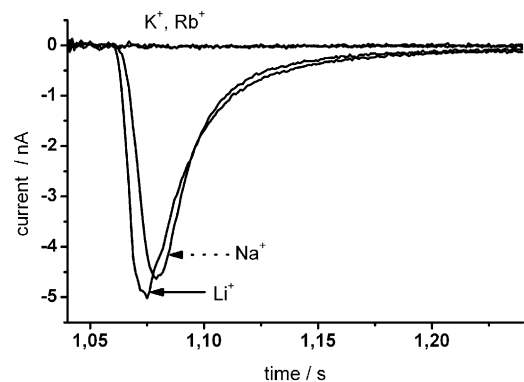

Fig. 4. Cation specificity of NhaA. Procedure was as in Fig. 3. The current traces recorded after 10 mM cation concentration jumps of Li$^+$, Na$^+$, K$^+$ and Rb$^+$ are shown. Proteoliposomes: as in Fig. 3. Buffer solution: 240 mM cholineCl, 25 mM Mops, 25 mM HEPES, 25 mM Tris, pH 8.0. In addition, the activating solution contained 10 mM of the cation, the nonactivating solution 10 mM cholineCl.

Na$^+$ and Li$^+$. Neither K$^+$ nor Rb$^+$ elicited current signals (within the system detection limits <20 pA).

3.5. Inhibitory effect of F$_v$-2C5 and 2-aminoperimidine

We have previously isolated three NhaA-specific mAbs (1F6, 2C5 and 5H4) which inhibit NhaA activity in proteoliposomes [18]. We used the mAb 2C5 F$_v$ fragment to confirm that the current measured is mediated by NhaA (Fig. 5A). First, a signal was recorded in the absence of the
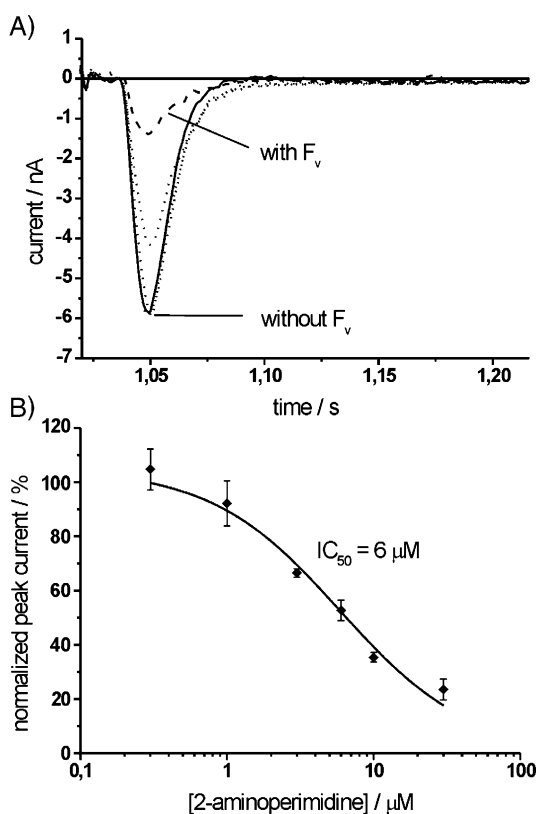

Fig. 5. Specific inhibition of NhaA: (A) Inhibitory effect of the monoclonal antibody fragment F$_v$-2C5. Signal generated by a 10 mM Na$^+$ concentration jump before (solid line) and after incubation (10 min) of the proteoliposomes adsorbed to the SSM with 25 μl containing 6.9 mg/ml F$_v$-2C5 (dashed line). The signal recovered after rinsing with antibody-free solution (dotted lines). For adsorption of proteoliposomes to the SSM 20 μl of NhaA proteoliposome solution (4.25 mg/ml lipids, LPR=21) was added to the cuvette. The buffer solution contained 10 mM KCl, 1 mM DTT, 100 mM Tris, 100 mM Mops, 100 mM HEPES, pH 8.0 (KOH). The activating and the nonactivating solution contained in addition 10 mM NaCl or 10 mM KCl, respectively. (B) Inhibitory effect of 2-aminoperimidine. Signals were generated by 10 mM Na$^+$ concentration jumps in the presence of different amounts of 2-aminoperimidine. Conditions as in (A) except for the following buffer solutions: 25 mM Tris, 25 mM HEPES, 50 mM KCl, 2 mM MgCl$_2$, pH 7.5 (KOH). The activating and the nonactivating solution contained in addition 10 mM NaCl or 10 mM KCl, respectively, and different concentrations of 2-aminoperimidine as indicated. The peak currents normalized to the current in the absence of inhibitor are plotted. The solid line is a fit using the function: $I=I_{max}(1-c/(IC_{50}+c))$ with the peak current I, the half maximum inhibitory concentration IC_{50} and the 2-aminoperimidine concentration c.

F$_v$. Then, the NhaA proteoliposomes adsorbed to the SSM were incubated with the F$_v$-2C5 fragment. A drastic inhibition of the Na$^+$ activated SSM current signal was observed. This inhibitory effect was reversible by rinsing with solution devoid of F$_v$-2C5. The strong inhibition by F$_v$-2C5, which is known to bind to a periplasmic epitope of NhaA, supports our conclusion that NhaA is preferentially RSO oriented in the proteoliposome preparations (see above).

It has recently been shown that the amiloride-like compound 2-aminoperimidine acts as a specific inhibitor of NhaA from *E. coli* [37]. Indeed, addition of micromolar concentrations of 2-aminoperimidine to the SSM suppressed the electrical signal generated by a 10 mM Na$^+$ concentration jump. An inhibition with an $IC_{50}=6$ μM was determined (Fig. 5B). This is somewhat larger than the value of 0.9 μM obtained previously from proton motive force-dependent Na$^+$/H$^+$ exchange measurements in isolated membrane vesicles [37]. Together, inhibition by the mAb 2C5 F$_v$ fragments as well as by the specific inhibitor 2-aminoperimidine proves that the recorded SSM current signals are due exclusively to the activity of NhaA.

3.6. Transient currents at different lipid to protein ratios of the reconstituted proteoliposomes

Transient currents generated by transporters on the SSM have been assigned in the past to a relatively fast electrogenic step followed by a rate limiting reaction [29,38]. If this interpretation holds also for the rapid decay of the NhaA mediated current (20 ms, Figs. 3 and 4), the decay represents transient kinetics of the transporter and the decay time constant is an upper bound for the relaxation time of the initial fast step. On the other hand, NhaA has an extremely high turnover (1000 s^{-1} at pH 8.0 [39]) suggesting that the recorded currents represent the steady state of the antiporter. Under these conditions, the decay of the current is brought about by the generation of an electrochemical potential across the liposomal membrane that gradually decreases the transport activity of NhaA. This can be tested by analyzing the time-dependent behavior of the recorded electrical currents using proteoliposomes with different lipid to protein ratios (LPR).

Transient currents after a Na$^+$ concentration jump at pH 8.5 and pH 7.0 using proteoliposomes with an LPR of 10 and 500 are compared in Fig. 6. The absolute peak currents of the recorded signals at LPR 10 and 500 were 3.4±2 nA and 0.2±0.1 nA measured on 8 different electrodes. The errors are large because the amount of adsorbed proteoliposomes varies from one experiment to the other. However, the amplitude ratio of ∼20 is consistent with the LPR of the two preparations within the error of the measurement. To facilitate the comparison of the time dependence in Fig. 6, the currents are
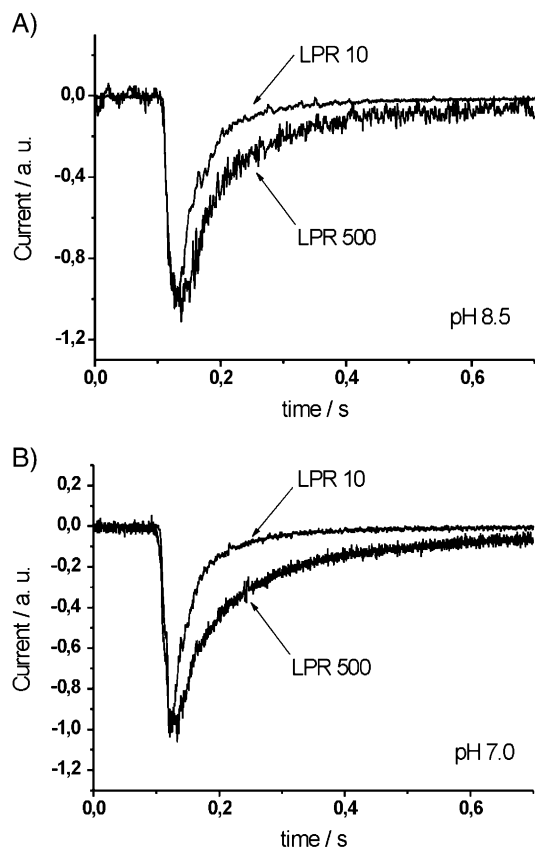
Fig. 6. Transient currents at different lipid to protein ratios. For comparison of their temporal behavior the transient currents were normalized to their respective maximal values. For adsorption of proteoliposomes to the SSM, 20 μl of NhaA proteoliposome solution (10 mg/ml lipids, LPR = 10 and 500) was added to the cuvette. (A) Transient currents at pH 8.5 after a 10 mM Na$^+$ concentration jump. Activating solution: 290 mM KCl, 10 mM NaCl. Nonactivating solution: 300 mM KCl. In addition, the buffers contained 5 mM MgCl$_2$, 25 mM HEPES, 25 mM Tris, pH 8.5 (KOH). The signals are recorded with a sample rate of 3 kHz (LPR 10) and 1 kHz (LPR 500). (B) Transient currents at pH 7.0 after a 100 mM Na$^+$ concentration jump. Activating solution: 200 mM KCl, 100 mM NaCl. Nonactivating solution: 300 mM KCl. In addition, the buffers contained 5 mM MgCl$_2$, 25 mM HEPES, 25 mM Tris, pH 7.0 (HCl). The signals are recorded with a sample rate of 3 kHz.

normalized to their peak values. Because the apparent K_m for Na$^+$ of NhaA is much lower at pH 8.5 a concentration jump of only 10 mM was used at pH 8.5 and one of 100 mM was used at pH 7.0. It is clear from the figure that both at pH 8.5 as well as at pH 7.0 the decay time constant of the electrical signal decreases with decreasing LPR, i. e., the more transporter is incorporated in the liposome the faster the current decays. The fact that the number of transporters determines the decay time constant rules out the possibility that this time constant reflects transient kinetic properties of the enzyme.

Taken together, these results indicate that the measured currents represent steady state turnover of the transporter at pH 8.0 as well as at pH 7.0. To a first approximation, the peak currents can, therefore, be used as a measure of enzymatic transport activity of NhaA.

3.7. Na$^+$ and Li$^+$ concentration dependence

The dependence of the current on the Na$^+$ concentration (in the range of 0.01 mM to 100 mM) was recorded at pH 8.5 and at pH 7.0. The peak currents obtained at different Na$^+$ concentrations are shown in Fig. 7A. To test whether charging of the liposomes affects the measured Na$^+$ affinity, we performed the measurement at different lipid to protein ratios (LPR) of the proteoliposomes. Both data sets, one using LPR = 10 and one using LPR = 500 yielded approximately the same Na$^+$ dependence with an apparent $K_m^{Na} = 11 \pm 0.7$ mM at pH 8.5. A similar experiment using proteoliposomes with LPR = 10 and LPR = 500 was performed at pH 7.0 and is shown in Fig. 7B. The Na$^+$
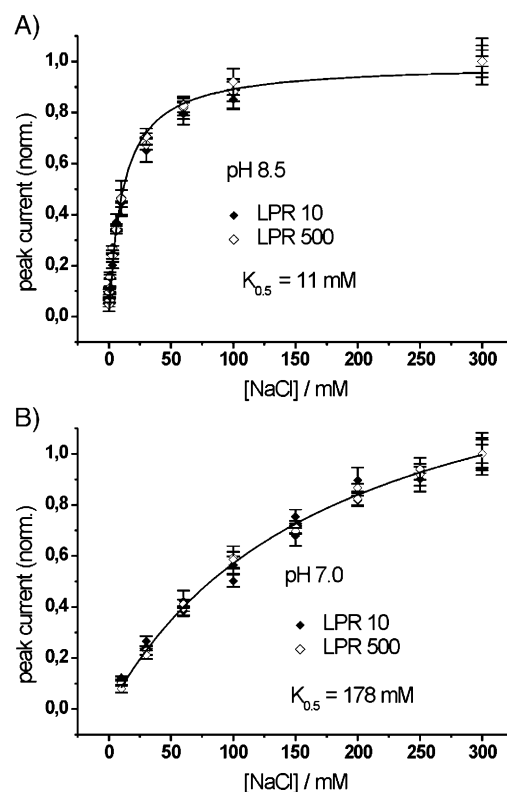

Fig. 7. Concentration dependence of the transient currents after a Na$^+$ concentration jump. Transient currents were measured at pH 8.5 and pH 7.0. For comparison, proteoliposomes with an LPR of 10 (solid symbols) and 500 (open symbols) were used. For each pH and LPR value, the concentration dependence was measured using two different sensors. Both are shown in the figure. The peak currents of each concentration dependence were normalized to V_{max} resulting from a hyperbolic fit to the individual data sets. The values given in the figure are average values of 3 subsequent recordings, error bars represent the standard error of the mean. For adsorption of proteoliposomes to the SSM 50 μl of NhaA, proteoliposome solution (1 mg/ml lipids, LPR = 10 or 500) was added to the cuvette. (A) Peak currents measured at pH 8.5. Activating solution: × mM NaCl, (300−×) mM KCl. Nonactivating solution: 300 mM KCl. In addition, the buffers contained 5 mM MgCl$_2$, 25 mM HEPES, 25 mM Tris, pH 8.5(KOH). (B) Peak currents measured at pH 7.0. Activating solution: × mM NaCl, (300−×) mM KCl. Nonactivating solution: 300 mM KCl. In addition, the buffers contained 5 mM MgCl$_2$, 25 mM HEPES, 25 mM Tris, pH 7.0 (HCl).

dependence determined in this case yielded a much higher value namely $K_m^{Na} = 178 \pm 10$ mM. Using Li$^+$ as the activating cation, we obtained (data not shown) $K_m^{Li} = 7.3$ mM at pH 8.0 and 51 mM at pH 7.0. These data demonstrate the higher affinity of the transporter for Li$^+$ in agreement with previous measurements [40].

3.8. pH dependence of wildtype and G338S NhaA

SSM measurements using NhaA proteoliposomes with concentration jumps of 10 and 100 mM NaCl were performed at various pH values from pH 6.5 to pH 10.0. Above pH 8.5 an irreversible decrease of the transient currents was observed. We, therefore, limited our analysis to pH values ≤8.5. The peak currents recorded were normalized to their maximal value at pH 8.3–8.5 and are displayed in Fig. 8. They increased from <0.01 nA at pH 6.5 to ~1.7 nA at pH 8.5 when a concentration jump of 10 mM is used. With a saturating concentration jump of 100 mM the increase of the peak current when going from pH 6.5 to pH 8.5 was only from ~0.15 nA to ~1.3 nA. This shows that the steady state turnover of NhaA at saturating Na$^+$ concentration increases by a factor of ~10 between 6.5 and
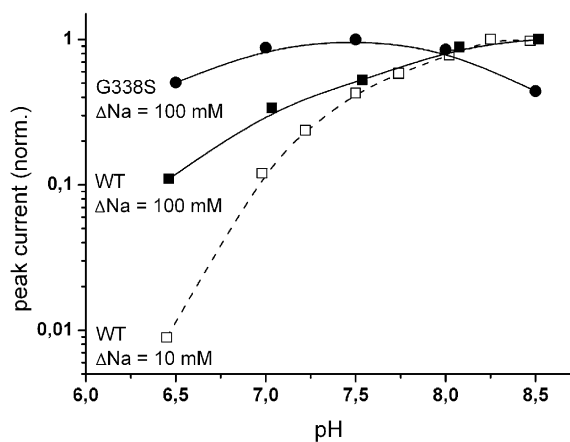

Fig. 8. pH dependence of the peak currents of wild-type NhaA and its mutant G338S. The measured peak currents were normalized to their maximal values at pH 8.3–8.5. NhaA wild type, ΔNa=10 mM (open squares). For adsorption of proteoliposomes to the SSM 10 μl of NhaA, proteoliposome solution (5 mg/ml lipids, LPR=3.4) was added to the cuvette. The buffer solution contained 290 mM KCl, 1 mM DTT, 25 mM Tris, 25 mM Mops, 25 mM HEPES, titrated with KOH (pH>7.3) or HCl (pH<7.3). In addition, the activating solution contained 10 mM NaCl, the nonactivating solution 10 mM KCl. NhaA wild type, ΔNa=100 mM (solid squares). For adsorption of proteoliposomes to the SSM 50 μl of NhaA proteoliposome solution (1 mg/ml lipids, LPR=10) was added to the cuvette. The buffer solution contained 5 mM MgCl$_2$, 200 mM KCl, 10 mM Citric acid, 10 mM HEPES, 10 mM Ches, titrated with KOH. In addition, the activating solution contained 100 mM NaCl, the nonactivating solution 100 mM KCl. NhaA G338S, ΔNa=100 mM (solid circles). For adsorption of proteoliposomes to the SSM 20 μl of NhaA proteoliposome solution (8.8 mg/ml lipids, LPR=17.5) was added to the cuvette. The buffer solution contained: 1 M cholineCl, 0.5 mM DTT, 25 mM Tris, 25 mM Mops, 25 mM HEPES, titrated with Tris (pH>7.3) or HCl (pH<7.3). In addition, the activating solution contained 100 mM NaCl, the nonactivating solution 100 mM cholineCl.

8.5 mM and by a factor of ~3 between 7.0 and 8.5 mM. The apparently much more pronounced upregulation in the 10-mM Na$^+$ jump experiment can be explained by the 10 fold lower affinity of the carrier at pH 7.0, which decreases the current of the 10 mM Na$^+$ jump experiment at pH 7.0 due to non-saturating substrate concentration.

The NhaA mutant G338S contains a single replacement of glycine 338 by serine. We have shown previously that this mutation alleviates the pH control of NhaA [13]. Here, we have further investigated G338S with the SSM method for comparison of its transport properties with those of the wild type protein. The pH dependence of the mutant G338S was determined by performing 100 mM Na$^+$ concentration jumps at various pH values from pH 6.5 to pH 8.5. The results summarized in Fig. 8 show that similar to the wild type protein, G338S is electrogenic under Na$^+$ gradient driven transport conditions, but its pH control is markedly changed. In contrast to the drastic increase in the activity of the wild type protein between pH 6.5 and pH 8.5, the mutation G338C results in almost constant activity between pH 6.5 and 8.5. Note that the measurement using the mutant enzyme were performed at saturating conditions, i.e. at 100 mM Na$^+$ and have, therefore, to be compared with the corresponding dependence of the wildtype (solid symbols in Fig. 8).

4. Discussion

Measuring various modes of the antiporter activity, the electrogenicity of NhaA Na$^+$/H$^+$ exchange has previously been deduced in cell-free systems of NhaA: In RSO membrane vesicles and NhaA-proteoliposomes, the membrane potential ΔΨ, negative inside, drives active Na$^+$ efflux [41–43] and passive downhill efflux of Na$^+$ creates ΔΨ, the dissipation of which accelerates the rate of downhill efflux of Na$^+$ [43]; in everted membrane vesicles, dissipation of ΔΨ accelerates the rate of Na$^+$ influx [44]; in fact, the creation of ΔΨ by the carrier rapidly inhibits its activity with a very fast kinetics that could not be resolved in the usual transport assays [20]. Therefore, the Na$^+$/2H$^+$ stoichiometry of NhaA in proteoliposomes could be estimated from the ratio between the rates of efflux of Na$^+$ and the coupled influx of H$^+$ directly only under conditions in which both components of the proton motive force Δμ$_{H^+}$ have been collapsed. Thus, an indirect thermodynamic approach was preferred for estimation of NhaA stoichiometry [39].

In the present study, electrogenicity of the Na$^+$/H$^+$ exchange of the NhaA antiporter has been demonstrated in proteoliposomes. This approach allows the investigation of the purified carrier in a defined environment and avoids interference with other cellular components. Two independent techniques have been employed: In the fluorescence measurements a potential negative inside was generated in the proteoliposomes upon a Na$^+$ concentration jump

(Fig. 1). Most importantly, translocation of positive charge out of the proteoliposomes was demonstrated directly by current measurements on NhaA proteoliposomes adsorbed to the SSM (Fig. 3). Transient currents were measured after a rapid solution exchange from a Na$^+$ (or Li$^+$) "free" to a Na$^+$ or (Li$^+$) containing solution. These currents were selectively inhibited by the NhaA-specific mAb fragment F_v-2C5 and by the specific inhibitor 2-aminoperimidine. Hence, this measurement represents the first direct evidence of electric current mediated by NhaA, proving directly the electrogenic activity of the NhaA Na$^+$/H$^+$ antiporter.

4.1. NhaA incorporates into liposomes in right side out orientation

Three independent experimental approaches demonstrate that the antiporter is predominantly RSO oriented in NhaA proteoliposomes: (a) All binding sites of NhaA for the NhaA-specific F_v fragment, F_v-2C5, were found exposed to the medium in NhaA proteoliposomes (Fig. 2A). (b) Accordingly the site-specific mAb fragment F_v-2C5 almost completely inhibited the current signal (Fig. 5). (c) The C-terminus of NhaA tagged with His-tag and factor Xa cleavable sites were found exposed to the internal volume of the proteoliposomes (Fig. 2B) and could only be cleaved after solubilization of the proteoliposomes by detergents (Fig. 2B).

It has been initially believed that during reconstitution into liposomes, membrane proteins insert in a mixed orientation into the lipid bilayer. However, an increasing number of cases in which the inserted proteins display a preferential orientation has been documented [45–48]. Apparently, structural asymmetry is important in the reconstitution process. Indeed, the 3D reconstruction of NhaA from cryo-electron microscopy analysis of highly ordered 2D crystals reveals a striking asymmetry between the two sides of NhaA [49].

Most importantly, the finding that NhaA is reconstituted in RSO orientation in proteoliposomes allows interpretation of the data of the electrical measurements in terms of vectorial transport properties of the antiporter and to compare our results with previous data, which have been obtained either with reconstituted NhaA in proteoliposomes [39,50] or in membrane vesicles [11,41].

A straightforward implication of the unidirectional incorporation of the NhaA protein in RSO orientation in the proteoliposomes is that the apparent K_m values determined in this study correspond to the periplasmic side of the carrier. In addition, the transport mode of NhaA studied here is the passive downhill uptake mode: a Na$^+$ concentration gradient directed inward (the Na$^+$ concentration jump) elicits, in agreement with the predicted Na$^+$/2H$^+$ antiport stoichiometry of NhaA [20], an inside negative potential as detected by fluorescence (Fig. 1) and electrical measurements (Fig. 3). This is the first study of the passive downhill uptake mode of NhaA in cell-free system.

4.2. The transient electrical signals represent stationary turnover of the NhaA antiporter in the passive downhill uptake mode

An interesting property of NhaA is its high turnover. Values up to 1000 s^{-1} at pH 8.0 [39] have been reported. Although an absolute quantitative analysis of enzyme activity is not possible using the SSM technique (because the amount of adsorbed proteoliposomes is unknown), it is obvious that the transient signals of NhaA were up to 10 times larger than those obtained with other transporters [29,38]. This suggests that the transient currents generated by NhaA at the SSM corresponds to the transport of many elementary charges, which leads to the conclusion that the observed currents probably reflect steady state turnover of NhaA. Additional support to this contention comes from the dependence of the transient currents on the LPR of the proteoliposomes. Here, a high protein content of the proteoliposomes leads to fast decay of the current due to charging of the liposomes. This is observed at pH 8.5 and at pH 7.0. Therefore, even at pH 7.0, when a low steady state turnover is observed in passive Na$^+$ efflux (10^{-1} s, [9]), the currents generated by the transporter are steady state currents. Slow turnover and fast relaxation into the steady state can be explained by a simple cyclic kinetic model consisting of a fast and a slow step. The slow step limits turnover, while the fast step leads to a fast relaxation into the steady state.

4.3. Substrate dependency

A large discrepancy is revealed when we compare the K_m for cation transport of NhaA at basic pH determined in our electrical measurements (K_m^{Na}=11 mM at pH 8.5, K_m^{Li}=7.3 mM at pH 8.0) with that available in the literature: Compare, e.g., K_m^{Na}=0.11 mM determined at pH 8.6 from ΔpH driven Na$^+$ uptake [39] and K_m^{Li}=0.06 mM determined at pH 8 from the effect of Li$^+$ on ΔpH as measured with acridine orange in everted membrane vesicles [51]. Most probably, the different transport mode and/or orientation of the exchanger in these experiments accounts for the discrepancy. No comparison can be made at neutral pH since K_m values for NhaA at neutral pH are not available in the literature.

It should be emphasized that all our measurements were performed on the passive downhill uptake mode of NhaA, a reversed transport mode with respect to the physiological activity of NhaA. The physiological role of NhaA is to excrete Na$^+$ in exchange for H$^+$ import to the cytoplasm to maintain intracellular pH constant [7]. Under growth conditions, the primary H$^+$ pump maintains an inward directed proton-motive force at the bacterial cytoplasmic membrane that drives NhaA-dependent Na$^+$ excretion in exchange for H$^+$ uptake [52]. Hence, the high K_m measured here at the external side of the membrane for Na$^+$ (and Li$^+$), which is at least 100-fold higher compared to that measured at the cytoplasmic face of the membrane, can have a physio-

logical significance for maintaining intracellular Na$^+$ low with respect to the environment by ensuring rapid discharge of Na$^+$ from its extracellular binding site.

4.4. pH regulation of NhaA

NhaA is strongly regulated by pH. As assessed by measuring passive ^{22}Na efflux, turnover of the enzyme increases by a factor of more than 1000 when raising the pH from pH 6.5 to pH 8.5 [39]. Furthermore, in our electrical measurements, we detected a significantly larger peak current upon a Na$^+$ concentration jump at alkaline pH (Fig. 8). However, the electrical measurements yield an increase of only 10-fold over the whole pH range when the pH was raised from 6.5 to 8.5 in the presence of saturating concentrations of NaCl (100 mM). One may argue that high turnover at alkaline pH leads to early saturation of the peak current due to liposome charging. However, experiments at different lipid to protein ratios yielded the same apparent K_m for Na$^+$ (Fig. 7A) indicating that liposome charging is not affecting the peak currents. Hence, it is evident that in the passive downhill uptake mode the antiporter has properties that differ significantly from those of the previously investigated efflux modes. In contrast to the efflux mode, where pH regulation changes mainly turnover (V_{max}, [11]), we find that in the passive downhill uptake mode apparent K_m as well as turnover, V_{max}, are affected. Both increase by approximately a factor of 10 when changing from neutral (pH 6.5–7.0) to basic (pH 8.5) conditions. This cannot be explained by a simple kinetic model of a cation binding reaction followed by a pH regulated rate limiting step. There, upregulation of the rate limiting step would either keep the apparent K_m at a constant value (when the binding equilibrium is fast) or even decrease it (when binding is slow) instead of increasing it. Our data suggest that at acidic pH a pH signal at the pH "sensor" triggers a structural change of NhaA that slows down the rate limiting step and at the same time increases the apparent K_m for Na$^+$ at the periplasmic side of the transporter.

It has been previously shown that replacement of glycine at position 338 by a serine yielded a variant with a complete loss of pH regulation [13]. We have used this mutant enzyme to test the pH dependence of the transient currents at different pH. As shown in Fig. 8, the peak currents produced by the mutant protein, only changed ~2-fold over the entire pH range (pH 6.5 to 8.5) shown in the (Fig. 8). This is in good agreement with a ~2-fold change, over similar pH range, determined from ΔpH driven Na$^+$ uptake and passive Na$^+$ efflux measurements [13] and demonstrates that G338 is important for the pH regulation of NhaA in both, the active efflux as well as the passive influx modes of NhaA.

Acknowledgements

References

[1] I.C. West, P. Mitchell, Proton/sodium ion antiport in *Escherichia coli*, Biochem. J. 144 (1974) 87–90.

[2] E. Padan, M. Venturi, Y. Gerchman, N. Dover, Na(+)/H(+) antiporters, Biochim. Biophys. Acta 1505 (2001) 144–157.

[3] J. Orlowski, S. Grinstein, Diversity of the mammalian sodium/proton exchanger SLC9 gene family, Pfluegers Arch. 447 (2004) 549–565.

[4] L. Counillon, J. Pouyssegur, The expanding family of eucaryotic Na(+)/H(+) exchangers, J. Biol. Chem. 275 (2000) 1–4.

[5] S. Wakabayashi, T. Pang, T. Hisamitsu, M. Shigekawa, The Sodium-Hydrogen Exchange, from Molecule to its Role in Disease, Kluwer Academic Publishers, Boston, 2003.

[6] E. Padan, S. Schuldiner, Bacterial Na+/H+ Antiporters-Molecular Biology, Biochemistry and Physiology, in: W.N. Konings, H.R. Kaback, J. Lolkema (Eds.), The Handbook of Biological Physics, Elsevier Science, Amsterdam, 1996, pp. 501–531.

[7] E. Padan, T.A. Krulwich, Sodium stress, in: G. Stortz, R. Hengge-Aronis (Eds.), Bacterial Stress Responses, ASM Press, Washington, DC, 2000, pp. 117–130.

[8] M. Venturi, E. Padan, Purification of NhaA Na+/H+ antiporter of Escherichia Coli for 3D and 2D crystallization, in: C. Hunte, G. Von Jagow, H. Schagger (Eds.), A Practical Guide to Membrane Protein Purification, Academic Press, Amsterdam, 2002, pp. 179–190.

[9] D. Taglicht, E. Padan, S. Schuldiner, Overproduction and purification of a functional Na+/H+ antiporter coded by nhaA (ant) from *Escherichia coli*, J. Biol. Chem. 266 (1991) 11289–11294.

[10] E. Padan, T. Tzubery, K. Herz, L. Kozachkov, L. Galili, NhaA of *Escherichia coli*, as a model of a pH regulated Na+/H+ antiporter, Biochim. Biophys. Acta 1658 (2004) 2–13.

[11] Y. Gerchman, Y. Olami, A. Rimon, D. Taglicht, S. Schuldiner, E. Padan, Histidine-226 is part of the pH sensor of NhaA, a Na+/H+ antiporter in *Escherichia coli*, Proc. Natl. Acad. Sci. U. S. A. 90 (1993) 1212–1216.

[12] A. Rimon, Y. Gerchman, Y. Olami, S. Schuldiner, E. Padan, Replacements of histidine 226 of NhaA-Na+/H+ antiporter of *Escherichia coli*. Cysteine (H226C) or serine (H226S) retain both normal activity and pH sensitivity, aspartate (H226D) shifts the pH profile toward basic pH, and alanine (H226A) inactivates the carrier at all pH values, J. Biol. Chem. 270 (1995) 26813–26817.

[13] A. Rimon, Y. Gerchman, Z. Kariv, E. Padan, A point mutation (G338S) and its suppressor mutations affect both the pH response of the NhaA-Na+/H+ antiporter as well as the growth phenotype of *Escherichia coli*, J. Biol. Chem. 273 (1998) 26470–26476.

[14] T. Tzubery, A. Rimon, E. Padan, Mutation E252C increases drastically the K_m for Na and causes an alkaline shift of the pH dependence of NhaA Na+/H+ antiporter of *Escherichia coli*, J. Biol. Chem. 279 (2004) 3265–3272.

[15] A. Rimon, T. Tzubery, L. Galili, E. Padan, Proximity of cytoplasmic and periplasmic loops in NhaA Na+/H+ antiporter of *Escherichia coli* as determined by site-directed thiol cross-linking, Biochemistry 41 (2002) 14897–14905.

[16] A. Rothman, Y. Gerchman, E. Padan, S. Schuldiner, Probing the conformation of NhaA, a Na+/H+ antiporter from *Escherichia coli*, with trypsin, Biochemistry 36 (1997) 14572–14576.

[17] Y. Gerchman, A. Rimon, E. Padan, A pH-dependent conformational change of NhaA Na(+)/H(+) antiporter of *Escherichia coli* involves loop VIII–IX, plays a role in the pH response of the protein, and is maintained by the pure protein in dodecyl maltoside, J. Biol. Chem. 274 (1999) 24617–24624.

[18] E. Padan, M. Venturi, H. Michel, C. Hunte, Production and characterization of monoclonal antibodies directed against native epitopes of NhaA, the Na+/H+ antiporter of *Escherichia coli*, FEBS Lett. 441 (1998) 53–58.

[19] M. Venturi, A. Rimon, Y. Gerchman, C. Hunte, E. Padan, H. Michel, The monoclonal antibody 1F6 identifies a pH-dependent conformational change in the hydrophilic NH_2 terminus of NhaA Na+/H+ antiporter of *Escherichia coli*, J. Biol. Chem. 275 (2000) 4734–4742.

[20] D. Taglicht, E. Padan, S. Schuldiner, Proton-sodium stoichiometry of NhaA, an electrogenic antiporter from *Escherichia coli*, J. Biol. Chem. 268 (1993) 5382–5387.

[21] H.A. Lester, S. Mager, M.W. Quick, J.L. Corey, Permeation properties of neurotransmitter transporters, Annu. Rev. Pharmacol. Toxicol. 34 (1994) 219–249.

[22] S. Mager, C. Min, D.J. Henry, C. Chavkin, B.J. Hoffman, N. Davidson, H.A. Lester, Conducting states of a mammalian serotonin transporter, Neuron 12 (1994) 845–859.

[23] S. Mager, Y. Cao, H.A. Lester, Measurement of transient currents from neurotransmitter transporters expressed in *Xenopus* oocytes, Methods Enzymol. 296 (1998) 551–566.

[24] A. Galli, R.D. Blakely, L.J. DeFelice, Patch-clamp and amperometric recordings from norepinephrine transporters: channel activity and voltage-dependent uptake, Proc. Natl. Acad. Sci. U. S. A. 95 (1998) 13260–13265.

[25] M.P. Kavanaugh, Neurotransmitter transport: models in flux, Proc. Natl. Acad. Sci. U. S. A. 95 (1998) 12737–12738.

[26] K. Seifert, K. Fendler, E. Bamberg, Charge transport by ion translocating membrane proteins on solid supported membranes, Biophys. J. 64 (1993) 384–391.

[27] T. Gropp, N. Brustovetsky, M. Klingenberg, V. Muller, K. Fendler, E. Bamberg, Kinetics of electrogenic transport by the ADP/ATP carrier, Biophys. J. 77 (1999) 714–726.

[28] J. Pintschovius, K. Fendler, Charge translocation by the Na+/K+-ATPase investigated on solid supported membranes: rapid solution exchange with a new technique, Biophys. J. 76 (1999) 814–826.

[29] C. Ganea, T. Pourcher, G. Leblanc, K. Fendler, Evidence for intraprotein charge transfer during the transport activity of the melibiose permease from *Escherichia coli*, Biochemistry 40 (2001) 13744–13752.

[30] Y. Olami, A. Rimon, Y. Gerchman, A. Rothman, E. Padan, Histidine 225, a residue of the NhaA-Na+/H+ antiporter of *Escherichia coli* is exposed and faces the cell exterior, J. Biol. Chem. 272 (1997) 1761–1768.

[31] G. Kleymann, C. Ostermeier, B. Ludwig, A. Skerra, H. Michel, Engineered Fv fragments as a tool for the one-step purification of integral multisubunit membrane protein complexes, Biotechnology (NY) 13 (1995) 155–160.

[32] J.F. Hoffman, P.C. Laris, Determination of membrane potentials in human and Amphiuma red blood cells by means of fluorescent probe, J. Physiol. 239 (1974) 519–552.

[33] M.N. Ivkova, V.A. Pechatnikov, V.G. Ivkov, Mechanism of fluorescent response of the probe diS-C3-(5) to transmembrane potential changes in a lecithin vesicle suspension, Gen. Physiol. Biophys. 3 (1984) 97–117.

[34] D. Taglicht, E. Padan, S. Schuldiner, Proton-sodium stoichiometry of NhaA, an electrogenic antiporter from *Escherichia coli*, J. Biol. Chem. 268 (1993) 5382–5387.

[35] M. Venturi, C. Hunte, Monoclonal antibodies for the structural analysis of the Na+/H+ antiporter NhaA from *Escherichia coli*, Biochim. Biophys. Acta (2003) 46–50.

[36] A. Rothman, E. Padan, S. Schuldiner, Topological analysis of NhaA, a Na+/H+ antiporter from *Escherichia coli*, J. Biol. Chem. 271 (1996) 32288–32292.

[37] P. Dibrov, A. Rimon, J. Dzioba, A. Winogradzki, Y. Shalitin, E. Padan, 2-Amionopyridine, a specific inhibitor of bacterial NhaA Na+/H+ antiporters, FEBS Lett. (2005) 373–378.

[38] A. Zhou, A. Wozniak, K. Meyer-Lipp, M. Nietschke, H. Jung, K. Fendler, Charge translocation during cosubstrate binding in the Na+/Proline transporter of *E. coli*, J. Membr. Biol. 343 (2004) 931–942.

[39] D. Taglicht, E. Padan, S. Schuldiner, Overproduction and purification of a functional Na+/H+ antiporter coded by nhaA (ant) from *Escherichia coli*, J. Biol. Chem. 266 (1991) 11289–11294.

[40] E. Padan, S. Schuldiner, Na+/H+ antiporters, molecular devices that couple the Na+ and H+ circulation in cells, J. Bioenerg. Biomembr. 25 (1993) 647–669.

[41] M. Bassilana, E. Damiano, G. Leblanc, Kinetic properties of Na+ antiport in *Escherichia coli* membrane vesicles. Effects of imposed electrical potential, proton gradient and internal pH, Biochemistry 23 (1984) 5288–5294.

[42] M. Bassilana, E. Damiano, G. Leblanc, Relationships between the Na+−H+ antiport activity and the components of the electrochemical proton gradient in *Escherichia coli* membrane vesicles, Biochemistry 23 (1984) 1015–1022.

[43] S. Schuldiner, H. Fishkes, Sodium-proton antiport in isolated membrane vesicles of *Escherichia coli*, Biochemistry 17 (1978) 706–710.

[44] J. Beck, B. Rosen, Cation/proton antiport systems in *Escherichia coli*: properties of the sodium/proton antiporter, Arch. Biochem. Biophys. 194 (1979) 208–214.

[45] J. Knol, K. Sjollema, B. Poolman, Detergent-mediated reconstitution of membrane proteins, Biochemistry 37 (1998) 16410–16415.

[46] H. Jung, S. Tebbe, R. Schmid, K. Jung, Unidirectional reconstitution and characterization of purified Na+/proline transporter of *Escherichia coli*, Biochemistry 37 (1998) 11083–11088.

[47] U. Fristedt, R. Weinander, H.S. Martinsson, B.L. Persson, Characterization of purified and unidirectionally reconstituted Pho84 phosphate permease of *Saccharomyces cerevisiae*, FEBS Lett. 458 (1999) 1–5.

[48] P. Van Gelder, F. Dumas, J.P. Rosenbusch, M. Winterhalter, Oriented channels reveal asymmetric energy barriers for sugar translocation through maltoporin of *Escherichia coli*, Eur. J. Biochem. 267 (2000) 79–84.

[49] K.A. Williams, Three-dimensional structure of the ion-coupled transport protein NhaA, Nature 403 (2000) 112–115.

[50] P.A. Dibrov, D. Taglicht, Mechanism of Na+/H+ exchange by *Escherichia coli* NhaA in reconstituted proteoliposomes, FEBS Lett. 336 (1993) 525–529.

[51] E. Padan, N. Maisler, D. Taglicht, R. Karpel, S. Schuldiner, Deletion of ant in *Escherichia coli* reveals its function in adaptation to high salinity and an alternative Na+/H+ antiporter system(s), J. Biol. Chem. 264 (1989) 20297–20302.

[52] E. Padan, S. Schuldiner, Molecular physiology of Na+/H+ antiporters, key transporters in circulation of Na+ and H+ in cells, Biochim. Biophys. Acta 1185 (1994) 129–151.